

Effects of postdeposition annealing on the dielectric properties of antiferroelectric lanthanum-doped lead zirconate stannate titanate thin films derived from pulsed laser deposition

Yingbang Yao, S. G. Lu, and Haydn Chen^{a)}

Department of Physics and Materials Science, City University of Hong Kong, Kowloon, Hong Kong

K. H. Wong

Department of Applied Physics, The Hong Kong Polytechnic University, Kowloon, Hong Kong

(Received 2 February 2004; accepted 15 August 2004)

Lanthanum-doped lead zirconate stannate titanate antiferroelectric thin films were deposited onto Pt-buffered silicon substrates using the pulsed laser deposition method. The deposition temperature was 570 °C. The postdeposition annealing process was carried out in an oxygen-flow tube furnace at temperatures ranging from 650 to 800 °C for a duration of 30 min; its effects were studied through the variations of the microstructure as well as the electrical and dielectric properties. It was found that an appropriate annealing process at temperatures above 700 °C could substantially improve the dielectric properties. However, annealing beyond 800 °C caused the film properties to deteriorate severely. Explanations were given with regard to the microstructure-property relationship. © 2004 American Institute of Physics.

[DOI: 10.1063/1.1804226]

I. INTRODUCTION

Lead-based antiferroelectric materials have been intensively studied for many years due to their promising applications in microelectronics as actuators, high-energy storage capacitors, etc. Many methods have been used to prepare the thin films of such materials including sol-gel, sputtering, pulsed laser deposition (PLD), etc. Lead loss has been a problem, which results in the formation of a low permittivity pyrochlore phase. Furthermore, oxygen deficiency has been found to enhance the pyrochlore phase formation. Consequently, various approaches had been exploited to achieve a pure perovskite phase such as using lead-excess precursors, annealing in oxygen-rich atmosphere, or adopting the rapid thermal annealing process. For the PLD process, employing lead-excess targets combined with postdeposition annealing in an oxygen-rich atmosphere has shown good results, which has been utilized in this study for the preparation of the lanthanum-doped lead zirconate stannate titanate (PLZST) antiferroelectric thin films.

The annealing process plays an important role in tailoring the properties of materials because of the thermally induced phase transformation or microstructure modifications. For the lead-based ferroelectric or antiferroelectric thin films, postdeposition annealing was generally required to convert the films from an amorphous or a pyrochlore-perovskite mixture into the desired perovskite phase. In general, the amorphous phase transforms first to a metastable pyrochlore-type structure (at 350–500 °C), which might then crystallize into the stable perovskite phase (at 500–700 °C).¹ It has been shown that even a small amount of remanent nanoscale crystallites or layers of pyrochlore are detrimental to the electri-

cal properties for these materials.² However, if the annealing temperature exceeds 700 °C, lead loss could become severe enough to cause the film to deteriorate.³ Moreover, high-temperature or prolonged annealing could also result in strains and/or form barrier layers at the film-substrate interfaces (induced by the interdiffusion between the film and the substrate), which could lead to the severe deterioration of the films⁴ as well.

Therefore, the annealing temperature and duration are key factors in the lead-based thin-film preparation process. We had embarked on the current study to investigate the postdeposition annealing effects on the perovskite phase crystallization, surface morphology, as well as the electrical and dielectric properties of the antiferroelectric $\text{Pb}_{0.97}\text{La}_{0.02}(\text{Zr}_{0.65}\text{Sn}_{0.28}\text{Ti}_{0.07})\text{O}_3$ (PLZST) thin films prepared by the PLD method.

II. EXPERIMENT

Ceramic targets of predetermined composition were fabricated by the conventional solid oxides reaction method, with the calcination temperature and sintering temperature of 800 and 1200 °C, respectively. An excess of 10 mol% PbO was added in the green state to compensate for the lead loss. The composition of the PLZST target was located in the tetragonal antiferroelectric range, close to the morphotropic phase boundary in the ternary phase diagram.

The configuration of the PLD facilities can be found elsewhere.⁵ The substrate temperature was kept at 570 °C under an oxygen pressure of 125 mTorr. The excimer laser was operated at 5 Hz with the laser energy of 200 mJ (corresponding to a laser fluence around 5 J/cm²). The working wavelength of the laser was 248 nm (KrF). The deposition duration was kept at 18 min for all the samples. After deposition, the films were subjected to the annealing process un-

^{a)}Author to whom correspondence should be addressed; electronic mail: aphchen@cityu.edu.hk

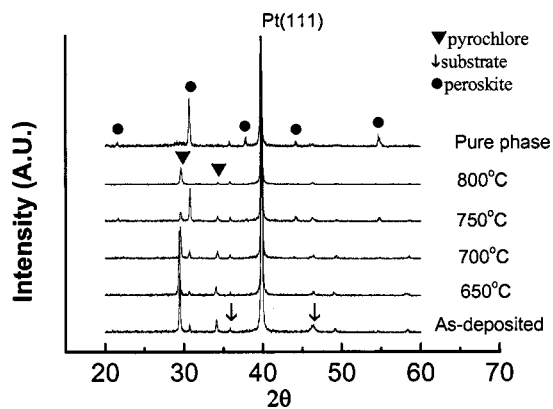


FIG. 1. XRD patterns for the as-deposited film and the annealed films, a pure phase pattern is shown.

der different temperatures, ranging from 650, 700, 750, to 800 °C for 30 min each in an oxygen-flow tube furnace. The heating rate was estimated to be 120 °C/min and the cooling rate was about 30 °C/min. The substrate used was a Pt-buffered silicon. For the pure phase PLZST thin films, the substrate temperature was 200 °C under an oxygen pressure of 100 mTorr. The laser density was 6 J/cm², with a repetition rate of 10 Hz. The deposition time was 12.5 min. The postdeposition annealing was performed at 650 °C for 30 min in an oxygen-flow ambient, using a tube furnace. Gold conductive pads of area of 0.0314 mm² were deposited on top of the PLZST samples by dc sputtering to facilitate the electrical property measurements.

The crystallographic phase was determined by x-ray diffraction (XRD) (Siemens D500 powder diffractometer). A field-emission scanning electron microscope (FESEM) (JOEL) was used to evaluate the surface morphology as well as the thickness of the films (by a cross-section view). The dielectric properties were measured using a Hewlett-Packard 4284A Precision LCR meter automatically with a Delta 9023 chamber as a temperature controller, all the systems were controlled by a computer. The polarization-electric field (P-E) loops of the films were tested using a Precision Pro ferroelectric test system (Radiant Technologies, Inc.) with a H100 series probe station (Signatone) as a sample stage.

III. RESULTS AND DISCUSSION

A. XRD patterns and SEM results

The x-ray diffraction patterns of the as-deposited film as well as the films that underwent annealing at different temperatures are shown in Fig. 1. For the as-deposited film, the pyrochlore phase dominated with a small fraction of the perovskite phase. The full width at half maximum of the pyrochlore (222) diffraction peak was 0.18° and that of the perovskite (110) peak was 0.13°, indicating that the grain size was larger for the perovskite phase in the as-deposited films. Even the vol% of the pyrochlore phase was much higher than that of the perovskite phase, as indicated by the integrated intensity of their strongest peaks.

After annealing at 650 or 700 °C, the pyrochlore phase still existed as the main phase in the films. The amount of perovskite phase started to increase with the further increase

of the annealing temperature, at the expense of the pyrochlore phase. As the annealing temperature increased to 750 °C, the perovskite phase became favored over the pyrochlore phase. Annealing at an even higher temperature, e.g., 800 °C, however showed a reverse trend; that is, the pyrochlore phase started to reappear at the expense of the perovskite phase. This effect is attributed to the severe lead loss during the high-temperature annealing, thus inducing the preferred growth of the lead-deficient pyrochlore phase. From these results, the annealing process at 750 °C was found to be the most suitable for the phase transformation from pyrochlore to perovskite—a fairly narrow window during the postdeposition annealing process.

It has been reported that even when an extra lead source was used, some PbO was always lost during annealing.⁶ On the other hand, lead loss started near 700 °C and increased with the annealing temperature and annealing duration for the lead-based ceramics.³ Hence, it is reasonable to assume that the lead loss would occur even at temperatures lower than 700 °C. We have also conducted a preliminary study on the postdeposition annealing process for the PLZST films deposited at a temperature as low as 200 °C, and the optimum annealing temperature was found to be 650 °C (the pure phase curve was the result shown in Fig 1, and we use it as a comparison for all the results reported in this work). The starting phase for these films was amorphous instead of the crystallized pyrochlore-perovskite mixture as shown for the present case. Therefore, the annealing process seems to be more efficient for the phase transformation from amorphous to perovskite than that from the crystallized pyrochlore phase. The main obstacle for the perovskite phase transformation was the lead loss during annealing at a sufficiently high temperature, which could trigger the growth of the perovskite phase from the pyrochlore phase and yet not too high to lose lead.

The morphology evolution for the films subjected to the annealing process under the different temperatures is shown in Fig. 2. It can be seen that the surface of the as-deposited films is smooth with little droplets, as shown in Fig. 2(a). After annealing at 650 °C, many round-shaped particles appeared and spread over the whole surface, as shown in Fig. 2(b). These particles were considered to be the pyrochlore structure from the XRD pattern; there was no sign of the perovskite phase growth at this stage. However, these particles were converted into the perovskite phase as the annealing temperature was raised to 700 °C, based upon the XRD data; its corresponding rosette-shaped microstructure is shown in Fig. 2(c). This rosette-shaped perovskite phase was also observed by the others;^{7,8} they were considered to be perovskite islands in a pyrochlore matrix. Increasing the annealing temperature further yielded the coalescence of the perovskite islands along with the decrease of the pyrochlore matrix, as illustrated in Fig. 2(d). However, for the 800 °C-annealed sample, the rosette structure diminished and the film turned into a cluster structure with many pores distributed uniformly in the film. The pores are attributed to the PbO evaporation or the releasing of the gas bubbles embedded in the films after annealing at a high temperature.⁷

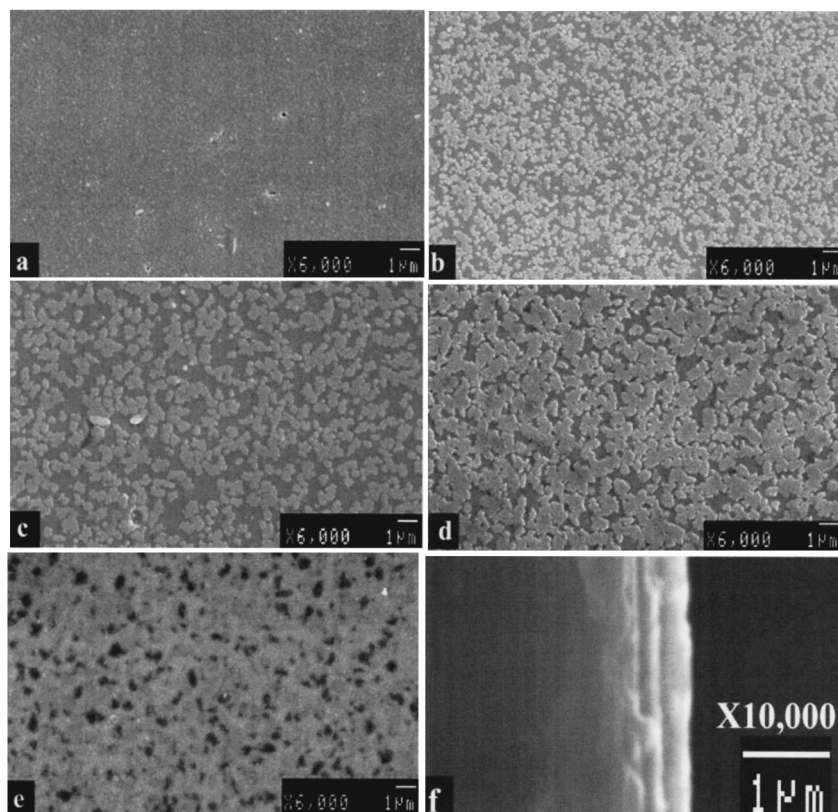


FIG. 2. FESEM plan view of the as-deposited film (a), and the films after annealing at 650 (b), 700 (c), 750 (d), and 800 °C (e); also, the cross-section view for the 650 °C-annealed sample (f).

The thickness of all the samples is around $0.33 \mu\text{m}$, as shown by the FESEM cross-section view of the 650 °C-annealed sample in Fig. 2(f).

B. Electrical and dielectric properties

The polarization hysteresis loops are illustrated in Fig. 3(a) for the as-deposited samples as well as for the films that underwent annealing (the film annealed at 800 °C showed electrical shortage so the results were not available.) As observed, the hysteresis loop for the as-deposited film is near the paraelectric type. This is ascribed to the large vol% of the pyrochlore phase in the film. As expected from the XRD and the microstructure results, after annealing at 650 °C, the saturation polarization increased and the 700 °C-annealed sample exhibited a hysteresis loop with the saturation polarization of $14 \mu\text{C}/\text{cm}^2$ with little remanent polarization. These features confirmed that a phase transformation from the pyrochlore to the perovskite has taken place after annealing. When the annealing temperature was increased to 750 °C, the hysteresis loop was well developed and the saturation polarization was increased to $23 \mu\text{C}/\text{cm}^2$. The remanent polarization for the film after annealing at 750 °C was $3 \mu\text{C}/\text{cm}^2$. However, the hysteresis loop did not show an obvious double hysteresis loop, although it was more delineated in its corresponding $C-V$ curve as shown in Fig. 3(b). This is probably due to the film composition located near the morphotropic phase boundary between the antiferroelectric and ferroelectric region. As such, a competition between antiferroelectricity and ferroelectricity could likely exist in the

film. Moreover, due to the tensile stress after cooling from the high annealing temperature, the ferroelectric phase could become even more stable.⁹ The cited factors could account for the observed remanent polarization as well as the smearing phase transitions between the antiferroelectric and the ferroelectric states under an electrical field as shown in Fig. 3(a). For the pure phase PLZST film, a double hysteresis loop was obtained, indicating the formation of an antiferroelectric phase. Its first derivative ($C-V$) [in Fig. 3(b)] had clear double peaks corresponding to the double hysteresis loops.

From these observations, it was concluded that the post-deposition annealing process could promote the phase transformation from pyrochlore to perovskite. An incomplete phase transformation to the perovskite phase would result in the degradation of the antiferroelectric properties of the film. Other features of the annealing process include the effects on the redistribution of defects,¹⁰⁻¹² the reconfiguration of the domain walls,¹³⁻¹⁵ or the elimination of the oxygen vacancies,¹⁶⁻¹⁸ etc. The defects and oxygen vacancies or lead vacancies are related to the leakage current and the dielectric relaxation with frequency, which are discussed in the following paragraphs.

Figure 4 shows the leakage current against the dc voltage for four sample conditions. At a low field, the ohmic conduction dominated whereas the space-charge-limited conduction (SCLC) prevailed under a high field, as observed in Fig. 4. There was an abrupt transition between the two regions and the turning point voltage, usually called the trap-

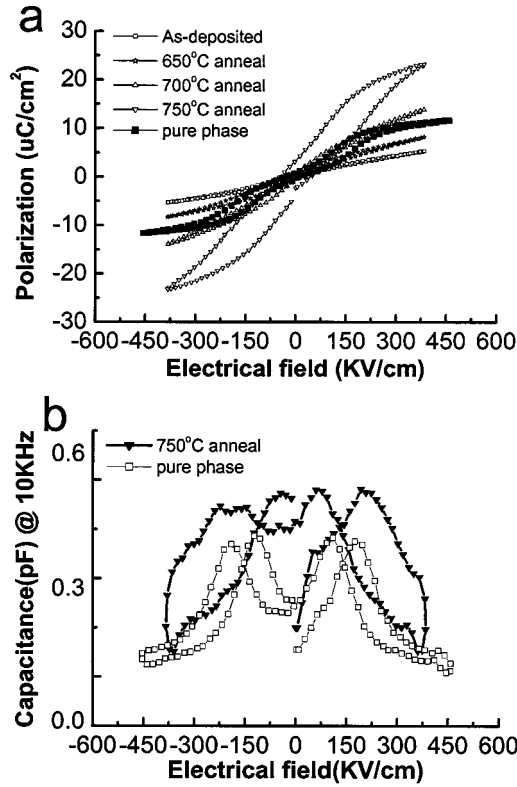


FIG. 3. Polarization hysteresis loops for the as-deposited and annealed films (a) and the corresponding $C-V$ curve for the 750 °C-annealed sample (b).

filled-level voltage V_{TFL} or onset voltage for the SCLC, was in the range of 2.2 V–2.6 V, corresponding to an electrical field of 67–79 KV/cm. It was interesting to find that the V_{TFL} for all the samples is almost the same within the accuracy of the measurements. The origin for the same values of V_{TFL} is possibly related to the similar deep levels of the electron traps located below the Fermi level.¹⁹ Another noticeable feature in the $I-V$ curves is the decrease of the leakage current with increasing the annealing temperature. In the ohmic conduction range, the leakage current decreases from 2.9×10^{-7} , 1.9×10^{-8} , and 3.8×10^{-9} to 1.2×10^{-9} A/cm² under an electrical field of 30 KV/cm (1 V) for the as deposited film and the annealed films with increasing the annealing temperature from 650 to 750 °C. In the SCLC range, there is little change, with the leakage current of the 750 °C-annealed sample being a bit larger than that of the

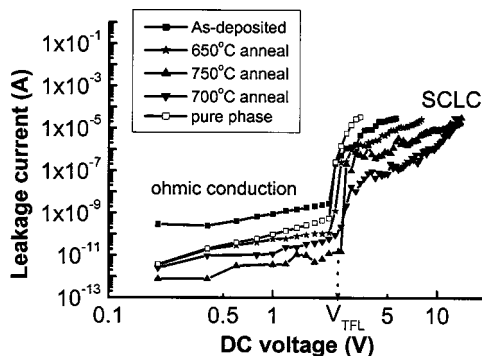


FIG. 4. Leakage current against dc voltage in a log-log plot.

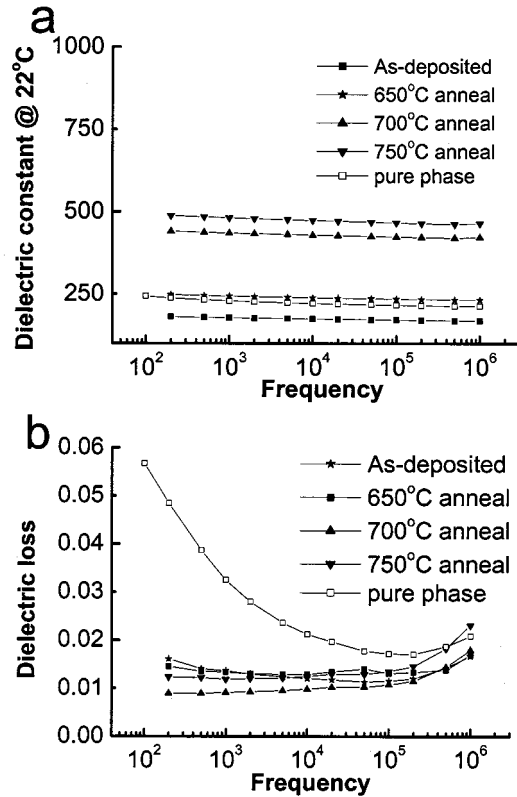


FIG. 5. Frequency-dependence of the dielectric constant (a) and dielectric loss (b), from 200 Hz to 1 MHz.

700 °C-annealed sample. This could have resulted from the more defects, such as lead vacancies, induced during the high temperature annealing.⁶ From the leakage current data, we can find that it is higher in the films composed mainly of the pyrochlore phase in comparison to the better-crystallized perovskite-phase-dominated films. The annealing process could pronoucnely suppress the leakage current as discussed previously. We noticed that the pure phase PLZST film did not show the smallest leakage current, which meant that the leakage current has no relation with the crystalline phase but the space charge near the surface or the grain boundaries.

The dielectric constant and dielectric loss against frequency are shown in Fig. 5. The measurements were performed at room temperature. As expected, the dielectric constant increased from 178 to 481 at 1 kHz after annealing at 750 °C. There was a large improvement in the dielectric constant when the films underwent annealing at 700 °C, as shown in Fig. 5(a). The dielectric losses for all the samples were confined in the range between 0.007 and 0.025 in the whole frequency domain studied. There was a weak low-frequency relaxation for the as deposited film and the 650 °C-annealed film. And this low-frequency dielectric dispersion disappeared after the film was annealed at 700 or 750 °C. Meanwhile, the dielectric loss decreased after annealing, as shown in Fig. 5(b). The decrease in the dielectric loss at low frequencies suggests the possible presence of a space-charge polarization.¹⁷ The higher dielectric constant and the lower dielectric loss of the films, subjected to annealing at temperatures of 700 and 750 °C, must be associated with a reduction of the nonferroelectric pyrochlore phase in

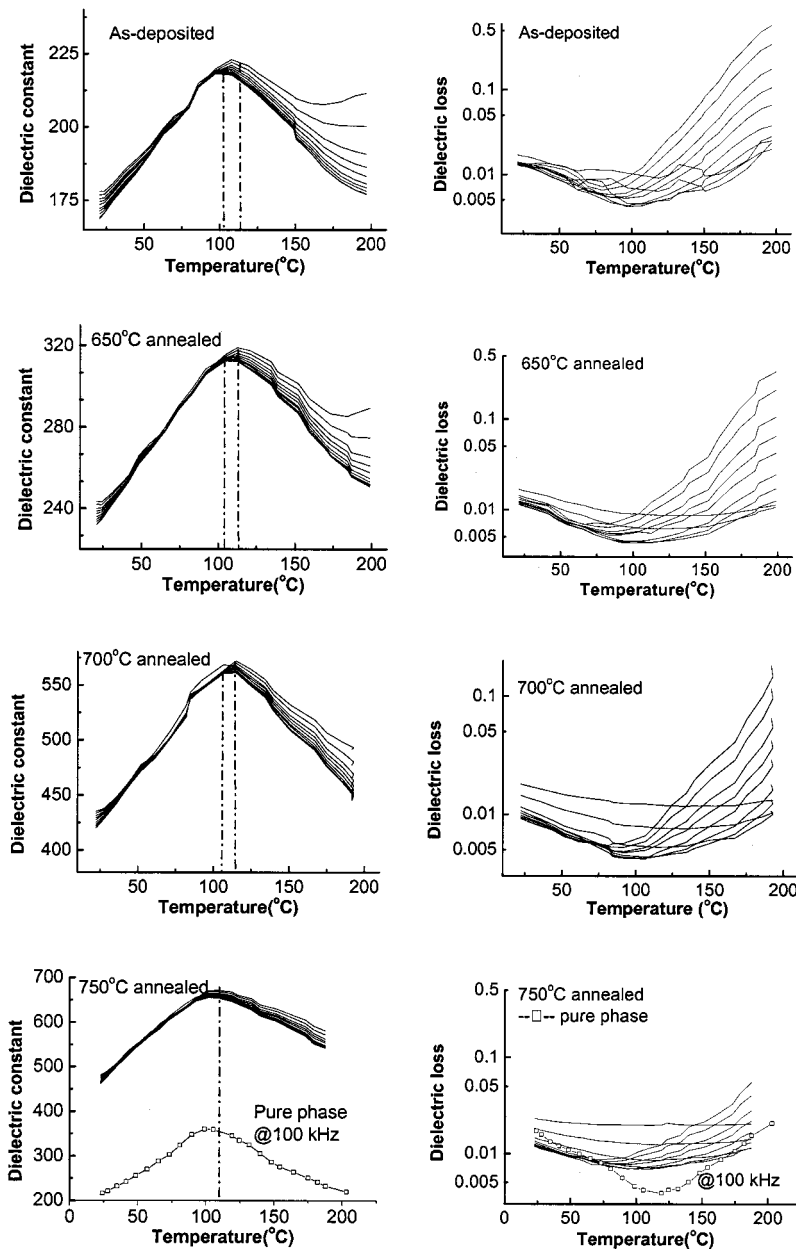


FIG. 6. Temperature dependence of the dielectric constant and dielectric loss of the as-deposited and annealed films.

the films. It is worth noting that the pure phase PLZST film has a dielectric constant comparable with that postannealed at 650 °C. It seems that the postannealing temperature has a prominent impact on the dielectric constant. However, the loss tangent of the pure phase PLZST was largest among all the films. The difference of the deposition temperature might be an indication of this phenomenon.

The temperature dependence of the dielectric constant as well as the dielectric loss is shown in Fig. 6. The measuring frequency ranged from 1 kHz to 1 MHz. The dielectric peak temperature for all the samples was found to be around 100 °C, which is consistent with that of the pure phase PLZST thin film shown in Fig. 6 for the 750 °C-postannealed film with the hollow square. There were two points to be noted: one is the frequency dispersion at temperatures beyond the dielectric peak temperature; the other is the slight frequency dependence of the dielectric peak temperature.

It is obvious that the frequency dispersion for the as-deposited films is much more severe in the temperature range higher than the dielectric peak temperature. In the perovskite structure, the cations are surrounded by a network of oxygen octahedra and are separated from the neighboring cations of the same kind (*A* or *B* site) by the entire unit cell (approximately 0.4 nm), thus making the movement of the cations difficult. However, the oxygen sites are about 0.28 nm apart, adjacent to one another and may thus move easier. This result has been confirmed by the measured higher diffusion coefficient of the oxygen vacancies in the BaTiO₃ perovskite structure.²⁰

Therefore, the frequency dispersion of the dielectric constant as well as the dielectric loss at higher temperatures is related to the oxygen vacancies.^{16–18,21} It was also reported that this kind of dispersion could be suppressed by using an oxygen-rich atmosphere annealing process.^{16,17} In our case, the annealing process in oxygen-flow environment also could

suppress the dielectric relaxation at high temperatures. Therefore, it is reasonable to reach the conclusion that after annealing at high temperatures, the concentration of oxygen vacancies decreased.

The frequency dependence of the dielectric peak temperature was observed in all the films except for the 750 °C-annealed one. The dielectric peak temperature shifted to a higher value as the frequency decreased. This is not a phenomenon of a relaxor, which shows a decreased dielectric peak temperature with the decreasing frequencies. After annealing at 750 °C, the frequency dependence of the dielectric peak temperature disappeared. Wu *et al.*¹⁶ also found such dielectric anomaly in SBT ceramics, which was thought to come from the oxygen-vacancy-related relaxation. In the present case, this concept could also be adopted to interpret the frequency dependence of the Curie temperature and its absence in the 750 °C-annealed sample. It is known that the oxygen vacancy concentration would change after annealing.²² So, the high-temperature oxygen-atmosphere annealing used herein suppressed the oxygen vacancy formation and finally eliminated the related dielectric relaxation¹⁸ after annealing at 750 °C.

IV. CONCLUSIONS

In summary, the postdeposition annealing process of the PLD-derived PLZST thin films was found to be important in the following aspects: (1) The phase transformation from pyrochlore to perovskite occurred efficiently as the annealing temperature went up to 750 °C, (2) the dielectric constant was enhanced and the dielectric loss was suppressed after annealing, and (3) the leakage current was decreased with the annealing temperature, whereas the trap-filled voltage was kept almost constant regardless of the annealing temperature.

ACKNOWLEDGMENTS

This work was supported in part by a RGC CERG grant (Grant No. 9040688) and in part by an internal grant (Grant No. 9380015) via the City University of Hong Kong. The authors would like to acknowledge the technical assistance from Mr. T. F. Hung and Mr. Daniel Yau, both from the City University of Hong Kong.

- ¹C. K. Kwok and S. B. Desu, *Ceram. Trans.* **25**, 85 (1992).
- ²J. Chen, A. Gorton, H. M. Chan, and M. P. Harmer, *J. Am. Ceram. Soc.* **69**, C303 (1986).
- ³F. Xia and X. Yao, *J. Mater. Sci.* **36**, 247 (2001).
- ⁴K. Sreenivas, *et al.*, *Ferroelectric Thin Films*, San Francisco, CA, 16–20 April 1990, edited by E. R. Myers and K. I. Kingon, [*Mater. Res. Soc. Symp. Proc.*] **200**, 255 (1990).
- ⁵W. Wu, K. H. Wong, C. L. Mak, C. L. Choy, and Y. H. Zhang, *J. Appl. Phys.* **88**, 2068 (2000).
- ⁶A. I. Kingon and J. B. Clark, *J. Am. Ceram. Soc.* **66**, 441 (1983).
- ⁷S. Y. Chen and I.-W. Chen, *J. Am. Ceram. Soc.* **81**, 97 (1998).
- ⁸S. H. Kim, J. G. Hong, S. K. Streiffer, and A. I. Kingon, *J. Mater. Res.* **14**, 1018 (1999).
- ⁹B. Xu, Y. Ye, and L. E. Cross, *J. Appl. Phys.* **87**, 2507 (1999).
- ¹⁰J. Mendiola, P. Ramos, and M. L. Calzada, *J. Phys. Chem. Solids* **59**, 1571 (1998).
- ¹¹R. Poyato, M. L. Calzada, and L. Pardo, *J. Appl. Phys.* **93**, 4081 (2003).
- ¹²R. Jimenez, M. L. Calzada, and J. Mendiola, *Thin Solid Films* **335**, 292 (1998).
- ¹³F. Xia and X. Yao, *J. Mater. Res.* **14**, 1683 (1999).
- ¹⁴F. Xia and X. Yao, *J. Appl. Phys.* **92**, 2709 (2002).
- ¹⁵H. Fan, G. T. Park, J. J. Choi, and H. E. Kim, *Appl. Phys. Lett.* **79**, 1658 (2001).
- ¹⁶Y. Wu, M. J. Forbess, S. Seraji, S. J. Limmer, T. P. Chou, and G. Cao, *J. Appl. Phys.* **89**, 5647 (2001).
- ¹⁷Y. Wu, M. Forbess, S. Seraji, S. Limmer, T. Chou, and G. Z. Cao, *J. Phys. D* **34**, 2665 (2001).
- ¹⁸C. Ang, Z. Yu, and L. E. Cross, *Phys. Rev. B* **62**, 228 (2000).
- ¹⁹S. S. N. Bharadwaja, and S. B. Krupanidhi, *J. Appl. Phys.* **86**, 5862 (1999).
- ²⁰L. Q. Zhou, O. M. Vilarinho and J. L. Baptista, *J. Am. Ceram. Soc.* **79**, 2436 (1996).
- ²¹O. Bidault, P. Goux, M. Kchikech, M. Belkaoui, and M. Maglione, *Phys. Rev. B* **49**, 7868 (1994).
- ²²M. Shen, Z. Dong, Z. Gan, S. Ge, and W. Cao, *Appl. Phys. Lett.* **80**, 2538 (2002).